

¹ Host Turkey B-cell Transcriptomics During THEV Infection
² Highlights Upregulated Cell Death and Breakdown Pathways
and Other Biological Processes
³

4

⁵ Abraham Quaye^{†,a}, Brett E. Pickett^a, Joel S. Griffitts^a, Bradford K. Berges^a, Brian D. Poole^{a,*}

⁶ ^aDepartment of Microbiology and Molecular Biology, Brigham Young University

⁷ †Primary Author

⁸ *Corresponding Author

9 Corresponding Author Information

¹⁰ brian_poole@byu.edu

11 Department of Microbiology and Molecular Biology,

¹² 4007 Life Sciences Building (LSB),

¹³ Brigham Young University,

14 Provo, Utah

15

16 **ABSTRACT**

17 **INTRODUCTION**

18 Turkey hemorrhagic enteritis virus (THEV), belonging to the family *Adenoviridae*, genus *Siadenovirus*,
19 infects turkeys, chickens, and pheasants (1, 2). Infecting its hosts via the feco-oral route, THEV causes
20 hemorrhagic enteritis (HE) in turkeys, a debilitating disease affecting predominantly 6-12-week-old turkey
21 pouls characterized by immunosuppression (IMS), depression, splenomegaly, intestinal lesions leading to
22 bloody droppings, and up to 80% mortality (3–6). The clinical disease usually persists in affected flocks for
23 about 7-10 days. However, secondary bacterial infections may extend the duration of illness and mortality for
24 an additional 2-3 weeks due to the immunosuppressive nature of the virus, exacerbating the economic losses
25 (5, 7). Low pathogenic (avirulent) strains of THEV have been isolated, which show subclinical infections
26 but retain the immunosuppressive effects. Since its isolation from a pheasant spleen, the Virginia Avirulent
27 Strain (VAS) has been used effectively as a live vaccine despite the immunosuppressive side-effects, but
28 the vaccinated birds are rendered more susceptible to opportunistic infections and death than unvaccinated
29 cohorts leading to significant economic losses (4, 5, 8–10).

30 It is well-established that THEV primarily infects and replicates in turkey B-cells of the bursa and spleen and
31 somewhat in macrophages, inducing apoptosis and necrosis. Consequently, a significant drop in number of
32 B-cells (specifically, IgM+ B-cells) and macrophages ensue along with increased T-cell counts with abnormal
33 T-cell subpopulation (CD4+ and CD8+) ratios. The cell death seen in the B-cells and macrophages is
34 generally proposed as the major cause of THEV-induced IMS as both humoral and cell-mediated immunity
35 are impaired (5, 6, 8, 11). It is also thought that the virus replication in the spleen attracts T-cells and
36 peripheral blood macrophages to the spleen where the T-cells are activated by cytokines from activated
37 macrophages and vice versa. The activated T-cells undergo clonal expansion and secrete interferons: type I
38 (IFN- α and IFN- β) and type II (IFN- γ) as well as tumor necrosis factor (TNF) while activated macrophages
39 secrete interleukin 6 (IL-6), TNF, and nitric oxide (NO), an antiviral agent with immunosuppressive properties.
40 The inflammatory cytokines released by T-cells and macrophages (e.g., TNF and IL-6) may also induce
41 apoptosis in bystander splenocytes, exacerbating the already numerous apoptotic and necrotic splenocytes,
42 culminating in IMS (8, 11) (see **Figure 1**). However, the precise molecular mechanisms of THEV-induced
43 IMS or pathways involved are poorly understood (6). Elucidating the specific mechanisms and pathways of
44 THEV-induced IMS is the most crucial step in THEV research as it will present a means of mitigating the IMS.
45 Next generation sequencing (NGS) is a groundbreaking technology that has significantly enhanced our
46 understanding of DNA and RNA structure and function and facilitated exceptional advancements in all
47 domains of biology and the Life Sciences (12). mRNA sequencing (RNA-seq), an NGS approach to
48 transcriptomic studies, is a versatile, high throughput, and cost-effective technology that allows a broad scan

49 of the entire transcriptome, thereby uncovering the active genes and molecular pathways and processes.
50 This technology has been leveraged in an ever increasing number of studies to elucidate active cellular
51 processes under a wide range of treatment conditions, including the transcriptomics of viral infections (12–16).
52 In RNA-seq studies, differentially expressed genes (DEGs) identified under different experimental conditions
53 are key to unlocking the interesting biology or mechanism under study. Identified DEGs are typically used for
54 functional enrichment analysis in large curated knowledgebases which connect genes to specific biological
55 processes, functions, and pathways such as gene ontology (GO) and Kyoto Encyclopedia of Genes and
56 Genomes (KEGG) pathways, shedding light on the biological question under study (17, 18).
57 To the best of our knowledge, no study has leveraged the wealth of information offered by RNA-seq to
58 elucidate the molecular mechanisms and pathways leading to THEV-induced IMS. To effectively counteract
59 the immunosuppressive effect of the vaccine, it is essential to unravel the host mechanisms/pathways
60 influenced by the virus to bring about IMS. In this study, we present the first transcriptomic profile of a
61 THEV infection using paired-end RNA-seq in a turkey B-cell line (MDTC-RP19), highlighting key host genes,
62 cellular/molecular processes and pathways affected during a THEV infection. Our RNA-seq yielded 149 bp
63 long high quality (mean PHRED Score of 36) sequences from each end of cDNA fragments, which were
64 mapped to the genome of domestic turkey (*Meleagris gallopavo*).

65 **RESULTS**

66 **Sequencing Results**

67 To identify the host transcriptome profile during THEV infection, MDTC-RP19 cells were THEV-infected
68 or mock-infected in triplicates or duplicates, respectively, and collected in like manner at 4-, 12-, 24-, and
69 72-hours post infection (hpi). mRNAs extracted from mock- or THEV-infected cells were sequenced on the
70 Illumina platform, yielding a total of **776.1** million raw reads (149 bp in length) across all samples (statistics
71 for the sequencing reads obtained from each RNA library are presented in **Table 1**). After trimming off
72 low-quality reads, the remaining **742.8** million total paired-end trimmed reads (approximately, **34.7-47.9**
73 million reads per sample) were mapped to the genome of *Meleagris gallopavo* obtained from the National
74 Center for Biotechnology Information (NCBI). The percentage of reads mapping to the host genome across
75 all samples ranged from **32.4-89.2%**. Although our sequencing reads have excellent quality scores (see
76 **Table 1**) at all time points, the DEGs identified at 4- and 72-hpi did not yield any results in the functional
77 enrichment analyses (i.e, GO term and KEGG pathway analysis); hence, they were excluded from all
78 subsequent analyses. In the remaining samples from 12- and 24-hpi, there is a high correlation was seen
79 between biological replicates (**Figure 2A and B**)

80 **DEGs of THEV-infected Versus Mock-infected Cells**

81 Gene expression levels were estimated with the StringTie software (19) in Fragments per kilobase of
82 transcript per million (FPKM) units. The analysis of DEGs was performed with the DESeq2 R package (20)
83 which employs negative binomial distribution model for read count comparisons. Using a P_{adjusted} -value
84 cutoff ≤ 0.05 as the inclusion criteria, a total of **2,343** and **3,295** genes were identified as differentially
85 expressed at 12-hpi and 24-hpi, respectively. ~~DEG analyses results at 12 and 24 hpi are presented in~~
86 ~~Supplementary Tables 1 and 2~~, respectively. At 12-hpi, **1,079** genes were upregulated and **1,264** genes
87 downregulated, whereas **1,512** genes were upregulated and **1,783** genes downregulated at 24-hpi (**Figure**
88 **2C**, and **Figure 3A-C**). The log₂fold-change(FC) values at 12-hpi ranged between **-1.4** and **+1.7** for **TMEM156**
89 (**Transmembrane Protein 156**) and **LIPG** (**Lipase G**), respectively. At 24-hpi, the log₂FC values ranged
90 between **-2.0** and **+2.6** for **C1QTNF12** (**C1q And TNF Related 12**) and **KCNG1** (**Potassium Voltage-Gated**
91 **Channel Modifier Subfamily G Member 1**), respectively.

92 **Functional Enrichment Analyses (GO, KEGG pathway, and interaction network analyses)**

93 Gene ontology (GO) enrichment analysis was performed for 12- and 24-hpi DEGs with the gprofiler2
94 (version **0.2.3**) R package (21), which outputs results in three GO categories – cellular components (CP),
95 biological processes (BP), and molecular functions (MF). Results with P_{adjusted} -value ≤ 0.05 were considered

96 functionally enriched. The GO enrichment analyses results at 12-hpi and 24-hpi showed significant similarities
97 among all three GO categories. At both time points, cellular breakdown processes were upregulated while
98 cellular maintenance processes and structures were downregulated in all three GO categories (**Table 2A-B**
99 and **Table 3A-B**).

100 For upregulated DEGs at 12-hpi, GO terms annotated under the biological processes (BP) category broadly
101 cluster into: apoptosis, catabolic processes, cellular metabolism, response to stimuli, and protein processing
102 (**Figure 4A**). Under the cellular components (CC) GO category, the GO terms relate with cytoplasmic
103 vacuolation while the GO terms under the molecular functions (MF) category broadly fit under protein
104 binding (**Table 2A**). For 12-hpi downregulated DEGs, the GO terms in BP category generally fall under:
105 translation, protein biosynthesis and folding; ribosome biogenesis; nitrogen compound metabolism; nucleic
106 acid synthesis, metabolism, processing, and replication; and energy metabolism (**Figure 4C**). As for the CC
107 category GO terms, they broadly group into: ribosome, mitochondria, respirosome, and nucleus while the
108 MF category GO terms generally belong to: translation regulator activity, protein folding chaperone, catalytic
109 activity (acting on a nucleic acids), and ATP hydrolysis activity (**Table 2B**).

110 At 24-hpi, the GO terms under the BP GO category for the upregulated DEGs are connected with: catabolic
111 process, protein ubiquitination and proteolysis, cell signalling, and cell metabolism (**Figure 4B**). The GO terms
112 of the CC category, similar to those identified at 12-hpi, are also related with cytoplasmic vacuolation. The
113 MF category GO terms group into: protein ubiquitination activity, acyltransferase activity, and macromolecule
114 binding activity (**Table 3A**). The GO terms for the downregulated DEGs are markedly similar to those at
115 12-hpi in all three GO categories. The BP category GO terms broadly group into: translation, peptide
116 biosynthesis and folding, ribosome biogenesis, aerobic respiration and ATP synthesis, and cell cycle process
117 and DNA replication (**Figure 4D**). The GO terms of the CC category group under: ribosome, organelle,
118 mitochondrion, nucleus and chromosomes while the MF category GO terms group into: structural constituent
119 of ribosome and translation regulator activity, catalytic activity acting on a nucleic acid and nucleic acid
120 binding, aminoacyl-tRNA ligase activity, and NAD binding (**Table 3B**).

121 KEGG analysis on the DEGs was performed using both the gprofiler2 R package (21) and the DAVID
122 (Database for Annotation, Visualization and Integrated Discovery; version 2021) online resource (22). Both
123 analysis resources gave similar results but the results from DAVID (**Table 4A**) includes more information
124 than the gprofiler2 results (**Table 4B**). The KEGG pathway analysis was congruent with the GO results,
125 revealing that generally, cell maintenance and upkeep pathways were downregulated while cell death and
126 breakdown pathways were upregulated. Cell maintenance pathways such as DNA replication and repair,
127 ribosome biogenesis, spliceosome, and oxidative phosphorylation were downregulated at 12-hpi. Similar

128 pathways were downregulated at 24-hpi. Cell breakdown pathways such as: autophagy, response to virus
129 (Influenza A), and steroid biosynthesis were upregulated at 12-hpi similar to 24-hpi, where pathways such
130 as: autophagy, ubiquitin-mediated proteolysis, lysosome, protein processing in endoplasmic reticulum, and
131 steroid biosynthesis were upregulated.

132 It is well-established that THEV induces cell death (apoptosis and necrosis) in infected B-cells, which is linked
133 to the IMS associated with THEV (8, 11, 23). Hence, we are particularly interested in cellular processes and
134 pathways associated with cell death and pathways that may affect the survivability of the host cells, thereby
135 accounting for THEV-induced IMS. We highlight the upregulated cell death (apoptosis and autophagy)
136 pathways, cellular metabolism, and responses to stimuli (especially ER-stress response) pathways identified
137 by our GO and KEGG analyses as the likely key aspects of THEV-host cell interaction leading to IMS.

138 **Cell Death and Breakdown Pathways Upregulated by THEV**

139 Many virus families, including adenoviruses, herpesviruses, poxviruses, baculoviruses, parvoviruses, retro-
140 viruses, rhabdoviruses, paramyxoviruses, orthomyxoviruses, togaviruses, and picornaviruses are known to
141 trigger apoptosis in infected host cells either by a direct action of a viral protein or due to the host antiviral
142 response (24–26). Adenoviruses generally possess the protein, E1B 19K to inhibit host cell apoptosis long
143 enough to complete their replication cycle (24, 26, 27). However, no such protein is known in THEV. A recent
144 paper showed several novel transcripts and open reading frames (ORFs) in the genome of THEV which
145 may offer a similar anti-apoptotic functions but the functions of these novel ORFs are yet to be shown (28).
146 Our data shows that apoptotic and autophagic pathways are upregulated during THEV infection, supporting
147 previous findings of apoptosis and necrosis of THEV-infected cells (8, 11, 23). For example, . . . , which are
148 proapoptotic, were upregulated.

149 **Cellular Metabolism Changes During THEV Infection**

150 Many viruses, such as hepatitis C virus, human cytomegalovirus, influenza virus, and rhinovirus, have been
151 documented to manipulate the cellular metabolism process for their use

152 **Cellular Responses to Stimuli during THEV infection**

153

154 **DISCUSSION**

155 We may not have seen a measurable immune response/pathway enrichment in the infected host cells
156 because the these B-cells may likely require other immune cells such as macrophages and T-cells for
157 activation/mount an immune response. Secondly, the curated data in the GO, and KEGG databases are
158 most complete for human and other model organisms; hence, there may not be enough information curated
159 for turkeys to highlight the anything that is not very strong immune response.

160 **CONCLUSIONS**

161 **MATERIALS AND METHODS**

162 **Cell culture and THEV Infection**

163 The Turkey B-cell line (MDTC-RP19, ATCC CRL-8135) was grown as a suspension culture in 1:1 complete
164 Leibovitz's L-15/McCoy's 5A medium with 10% fetal bovine serum (FBS), 20% chicken serum (ChS), 5%
165 tryptose phosphate broth (TPB), and 1% antibiotic solution (100 U/mL Penicillin and 100 μ g/mL Streptomycin),
166 at 41°C in a humidified atmosphere with 5% CO₂. Infected cells were maintained in 1:1 serum-reduced
167 Leibovitz's L15/McCoy's 5A media (SRLM) with 2.5% FBS, 5% ChS, 1.2% TPB, and 1% antibiotic solution. A
168 commercially available THEV vaccine was purchased from Hygieia Biological Labs (VAS strain). The stock
169 virus was titrated using an in-house qPCR assay with titer expressed as genome copy number (GCN)/mL,
170 similar to Mahshoub *et al* (29). Cells were THEV-infected or mock-infected in triplicates or duplicates,
171 respectively at a multiplicity of infection (MOI) of 100 GCN/cell, incubated at 41°C for 1 hour, and washed
172 three times with phosphate buffered saline (PBS) to get rid of free virus particles. At each time point (4-, 12-,
173 24-, and 72-hpi), triplicate (THEV-infected) and duplicate (mock-infected) samples were harvested for total
174 RNA extraction.

175 **RNA extraction and Sequencing**

176 Total RNA was extracted from infected cells using the Thermo Fisher RNAqueous™-4PCR Total RNA Isolation
177 Kit (which includes a DNase I digestion step) per manufacturer's instructions. An agarose gel electrophoresis
178 was performed to check RNA integrity. The RNA quantity and purity was initially assessed using nanodrop,
179 and RNA was used only if the A260/A280 ratio was 2.0 ± 0.05 and the A260/A230 ratio was >2 and <2.2.
180 Extracted total RNA samples were sent to LC Sciences, Houston TX for poly-A-tailed mRNA sequencing.
181 RNA integrity was checked with Agilent Technologies 2100 Bioanalyzer High Sensitivity DNA Chip and
182 poly(A) RNA-seq library was prepared following Illumina's TruSeq-stranded-mRNA sample preparation
183 protocol. Paired-end sequencing, generating 150 bp reads was performed on the Illumina NovaSeq 6000
184 sequencing system. The paired-end 150bp sequences obtained during this study and all expression data
185 have been submitted to the Gene Expression Omnibus database, under accession no #####

186 **Quality Control and Mapping Process**

187 Sequencing reads were processed following a well-established protocol described by Pertea *et al* (19),
188 using Snakemake - version 7.32.4 (30), a popular workflow management system to drive the pipeline.
189 Briefly, raw sequencing reads were trimmed with Cutadapt - version 1.10 (31) and the quality of trimmed
190 reads evaluated using the FastQC software, version 0.12.1 (Bioinformatics Group at the Babraham Institute,
191 Cambridge, United Kingdom; www.bioinformatics.babraham.ac.uk), achieving an overall Mean Sequence
192 Quality (PHRED Score) of 36. Trimmed reads were mapped the reference *Meleagris gallopavo* genome

193 (https://ftp.ncbi.nlm.nih.gov/genomes/all/GCF/000/146/605/GCF_000146605.3_Turkey_5.1/GCF_000146
194 605.3_Turkey_5.1_genomic.fna.gz) with Hisat2 - version 2.2.1 (19) using the accompanying gene transfer
195 format (GTF) annotation file (https://ftp.ncbi.nlm.nih.gov/genomes/all/GCF/000/146/605/GCF_000146605.3
196 _Turkey_5.1/GCF_000146605.3_Turkey_5.1_genomic.gtf.gz) to build a genomic index. Samtools - version
197 1.19.2 was used to convert the output Sequence Alignment Map (SAM) file to the more manageable Binary
198 Alignment Map (BAM) format. The StringTie (v2.2.1) software (19), set to expression estimation mode was
199 used to generate normalized gene expression estimates from the BAM files for genes in the reference GTF
200 file after which the prepDE.py3 script was used to extract read count information from the StringTie gene
201 expression files, providing an expression-count matrix for downstream DEG analysis.

202 **DEG Analysis and Functional Enrichment Analysis**

203 DEG analysis between mock- and THEV-infected samples was performed using the very popular DESeq2
204 (20), which employs a Negative Binomial distribution model for read count comparisons. Genes with P_{adjusted} -
205 value ≤ 0.05 were considered as differentially expressed. The read count data are deposited at Gene
206 Expression Omnibus (GEO) under accession number ###. The functional profiling of DEGs (GO and KEGG
207 analyses) were performed based on GO databases and KEGG databases using the R package gprofiler2
208 (21) with *Meleagris gallopavo* as the reference organism. Results with P_{adjusted} -value ≤ 0.05 were included
209 as functionally enriched. Additionally, the DAVID (Database for Annotation, Visualization and Integrated
210 Discovery; version 2021) online analysis tool was used for KEGG pathway analysis. All visualization plots
211 were made using ggplot2, pheatmap, and ggvenn R packages (32–34).

212 **Validation of DEGs by Reverse Transcriptase Quantitative PCR (RT-qPCR)**

213 **Statistical Analysis**

²¹⁴ **DATA AVAILABILITY**

215 **CODE AVAILABILITY**

216 **ACKNOWLEDGMENTS**

217 **REFERENCES**

- 218 1. Harrach B. 2008. Adenoviruses: General features, p. 1–9. In Mahy, BWJ, Van Regenmortel, MHV
(eds.), Encyclopedia of virology (third edition). Book Section. Academic Press, Oxford.
- 219 2. Davison A, Benko M, Harrach B. 2003. Genetic content and evolution of adenoviruses. The Journal
of general virology 84:2895–908.
- 220 3. Gross WB, Moore WE. 1967. Hemorrhagic enteritis of turkeys. Avian Dis 11:296–307.
- 221 4. Beach NM. 2006. Characterization of avirulent turkey hemorrhagic enteritis virus: A study of the
molecular basis for variation in virulence and the occurrence of persistent infection. Thesis.
- 222 5. Dhamma K, Gowthaman V, Karthik K, Tiwari R, Sachan S, Kumar MA, Palanivelu M, Malik YS, Singh
RK, Munir M. 2017. Haemorrhagic enteritis of turkeys – current knowledge. Veterinary Quarterly
37:31–42.
- 223 6. Tykałowski B, Śmiałek M, Koncicki A, Ognik K, Zduńczyk Z, Jankowski J. 2019. The immune response
of young turkeys to haemorrhagic enteritis virus infection at different levels and sources of methionine
in the diet. BMC Veterinary Research 15.
- 224 7. Pierson F, Fitzgerald S. 2008. Hemorrhagic enteritis and related infections. Diseases of Poultry
276–286.
- 225 8. Rautenschlein S, Sharma JM. 2000. Immunopathogenesis of haemorrhagic enteritis virus (HEV) in
turkeys. Dev Comp Immunol 24:237–46.
- 226 9. Larsen CT, Domermuth CH, Sponenberg DP, Gross WB. 1985. Colibacillosis of turkeys exacerbated
by hemorrhagic enteritis virus. Laboratory studies. Avian Dis 29:729–32.

- 227 10. Beach NM, Duncan RB, Larsen CT, Meng XJ, Sriranganathan N, Pierson FW. 2009. Persistent infection of turkeys with an avirulent strain of turkey hemorrhagic enteritis virus. *Avian Diseases* 53:370–375.
- 228 11. Rautenschlein S, Suresh M, Sharma JM. 2000. Pathogenic avian adenovirus type II induces apoptosis in turkey spleen cells. *Archives of Virology* 145:1671–1683.
- 229 12. Satam H, Joshi K, Mangrolia U, Waghoo S, Zaidi G, Rawool S, Thakare RP, Banday S, Mishra AK, Das G, Malonia SK. 2023. Next-generation sequencing technology: Current trends and advancements. *Biology* 12:997.
- 230 13. Pandey D, Onkara Perumal P. 2023. A scoping review on deep learning for next-generation RNA-seq. Data analysis. *Functional & Integrative Genomics* 23.
- 231 14. Wang B, Kumar V, Olson A, Ware D. 2019. Reviving the transcriptome studies: An insight into the emergence of single-molecule transcriptome sequencing. *Frontiers in Genetics* 10.
- 232 15. Choi SC. 2016. On the study of microbial transcriptomes using second- and third-generation sequencing technologies. *Journal of Microbiology* 54:527–536.
- 233 16. Mo Q, Feng K, Dai S, Wu Q, Zhang Z, Ali A, Deng F, Wang H, Ning Y-J. 2023. Transcriptome profiling highlights regulated biological processes and type III interferon antiviral responses upon crimean-congo hemorrhagic fever virus infection. *Virologica Sinica* 38:34–46.
- 234 17. Ashburner M, Ball CA, Blake JA, Botstein D, Butler H, Cherry JM, Davis AP, Dolinski K, Dwight SS, Eppig JT, Harris MA, Hill DP, Issel-Tarver L, Kasarskis A, Lewis S, Matese JC, Richardson JE, Ringwald M, Rubin GM, Sherlock G. 2000. Gene ontology: Tool for the unification of biology. *Nature Genetics* 25:25–29.
- 235 18. Kanehisa M. 2000. KEGG: Kyoto encyclopedia of genes and genomes. *Nucleic Acids Research* 28:27–30.

- 236 19. Pertea M, Kim D, Pertea GM, Leek JT, Salzberg SL. 2016. Transcript-level expression analysis of RNA-seq experiments with HISAT, StringTie and ballgown. *Nature Protocols* 11:1650–1667.
- 237 20. Love MI, Huber W, Anders S. 2014. Moderated estimation of fold change and dispersion for RNA-seq data with DESeq2. *Genome Biology* 15:550.
- 238 21. Kolberg L, Raudvere U, Kuzmin I, Vilo J, Peterson H. 2020. gprofiler2— an r package for gene list functional enrichment analysis and namespace conversion toolset g:profiler. *F1000Research* 9 (ELIXIR).
- 239 22. Sherman BT, Hao M, Qiu J, Jiao X, Baseler MW, Lane HC, Imamichi T, Chang W. 2022. DAVID: A web server for functional enrichment analysis and functional annotation of gene lists (2021 update). *Nucleic Acids Research* 50:W216–W221.
- 240 23. Saunders GK, Pierson FW, Hurk JV van den. 1993. Haemorrhagic enteritis virus infection in turkeys: A comparison of virulent and avirulent virus infections, and a proposed pathogenesis. *Avian Pathology* 22:47–58.
- 241 24. Barber GN. 2001. Host defense, viruses and apoptosis. *Cell Death & Differentiation* 8:113–126.
- 242 25. Hardwick JM. 1997. Virus-induced apoptosis, p. 295–336. *In Apoptosis - pharmacological implications and therapeutic opportunities*. Elsevier.
- 243 26. Verburg SG, Lelievre RM, Westerveld MJ, Inkol JM, Sun YL, Workenhe ST. 2022. Viral-mediated activation and inhibition of programmed cell death. *PLOS Pathogens* 18:e1010718.
- 244 27. Ezoe H, Fatt RB, Mak S. 1981. Degradation of intracellular DNA in KB cells infected with cyt mutants of human adenovirus type 12. *Journal of Virology* 40:20–27.
- 245 28. Quaye A, Pickett BE, Griffitts JS, Berges BK, Poole BD. 2024. Characterizing the splice map of turkey hemorrhagic enteritis virus. *Virology Journal* 21.

- ²⁴⁶ 29. Mabsoub HM, Evans NP, Beach NM, Yuan L, Zimmerman K, Pierson FW. 2017. Real-time PCR-based infectivity assay for the titration of turkey hemorrhagic enteritis virus, an adenovirus, in live vaccines. *Journal of Virological Methods* 239:42–49.
- ²⁴⁷ 30. Mölder F, Jablonski KP, Letcher B, Hall MB, Tomkins-Tinch CH, Sochat V, Forster J, Lee S, Twardziok SO, Kanitz A, Wilm A, Holtgrewe M, Rahmann S, Nahnsen S, Köster J. 2021. Sustainable data analysis with snakemake. *F1000Research* 10:33.
- ²⁴⁸ 31. Martin M. 2011. Cutadapt removes adapter sequences from high-throughput sequencing reads. *EMBnetjournal* 17:10.
- ²⁴⁹ 32. Wickham H. 2016. *ggplot2: Elegant graphics for data analysis*. Springer-Verlag New York. <https://ggplot2.tidyverse.org>.
- ²⁵⁰ 33. Kolde R. 2019. *Pheatmap: Pretty heatmaps*. <https://CRAN.R-project.org/package=pheatmap>.
- ²⁵¹ 34. Yan L. 2023. *Ggvenn: Draw venn diagram by 'ggplot2'*. <https://CRAN.R-project.org/package=ggvenn>.

252 TABLES AND FIGURES

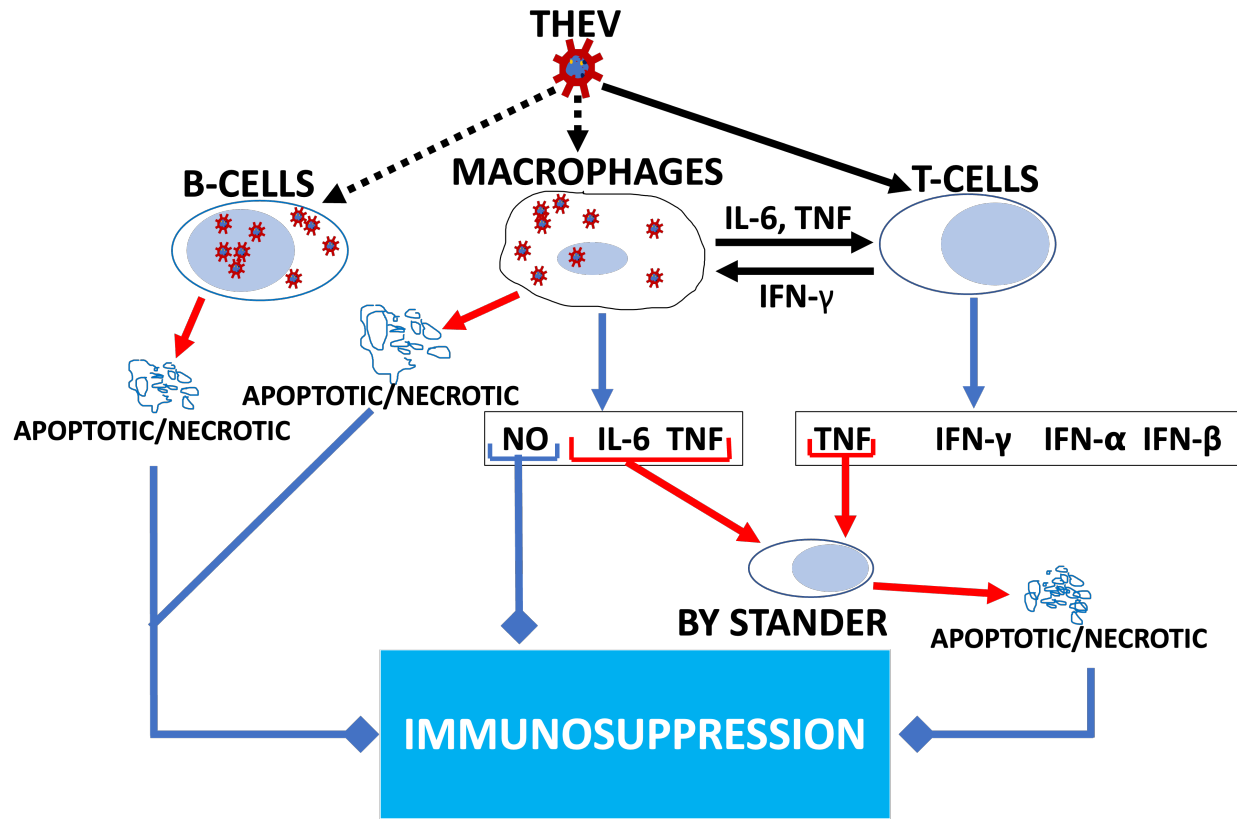


Figure 1: Model of THEV-induced immunosuppression in turkeys. THEV infection of target cells is indicated with black dotted arrows. Black unbroken arrows indicate cell activation. Red arrows indicate signals leading to apoptosis. Blue arrows indicate all cytokines released by the cell. Blue arrows with square heads indicate an event leading to IMS. Adapted from Rautenschlein *et al.* (8).

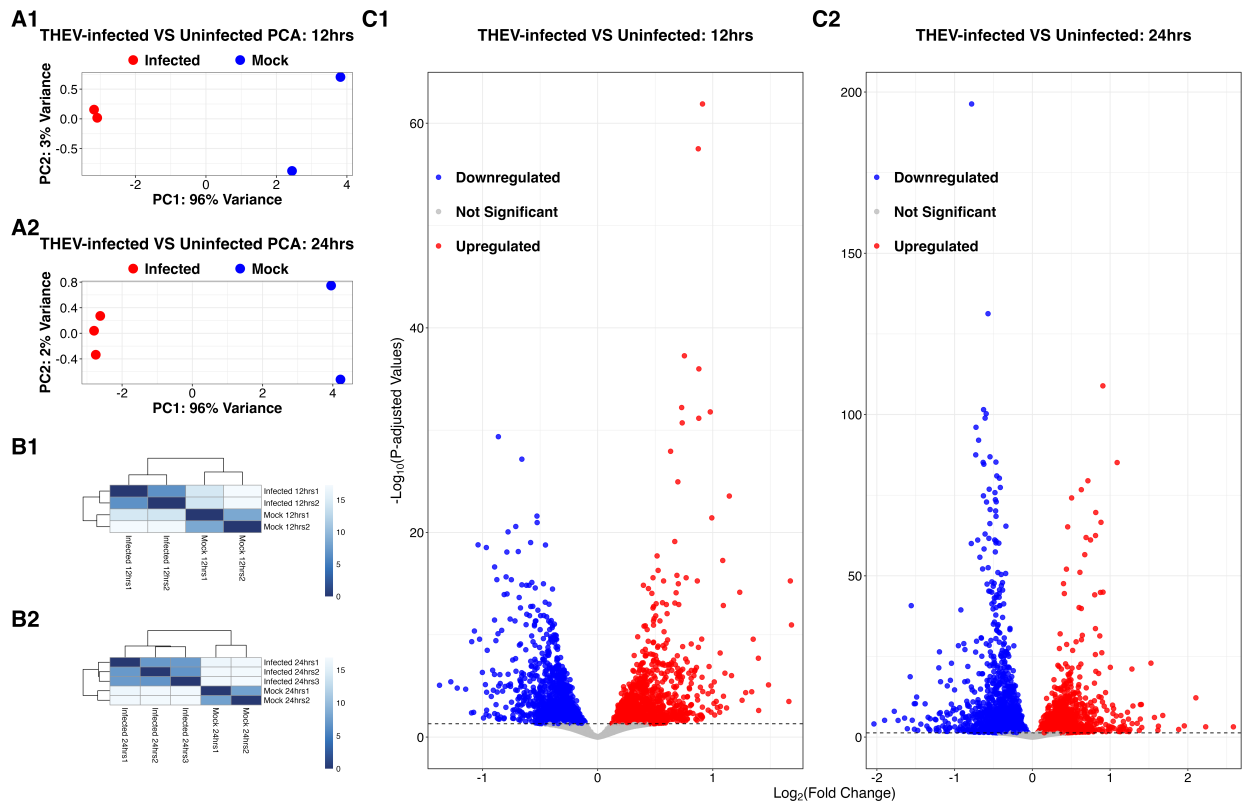


Figure 2. (A) Principal component analysis (PCA) of turkey B-cells during THEV infection. At 12-hpi (**A1**), the results indicate that the first (PC1) and second (PC2) principal components account for 96% and 3% of the variation in the samples, respectively. Whereas PC1 and PC2 account for 96% and 2% of the variation, respectively at 24-hpi (**A2**). **(B) Poisson distance matrices illustrating the RNA-seq library integrity within treatment (infected versus mock) groups.** The color scale represents the distances between biological replicates for both 12-hpi samples (**B1**) and 24-hpi samples (**B2**). Dark colors represent high correlation (similarity) between the samples involved. **(C) Volcano plots of DEGs between THEV-infected versus mock-infected cells at 12- and 24-hpi.** Red, blue, and grey dots represent upregulated, downregulated, and non-significant genes, respectively for both 12-hpi samples (**C1**) and 24-hpi samples (**C2**).

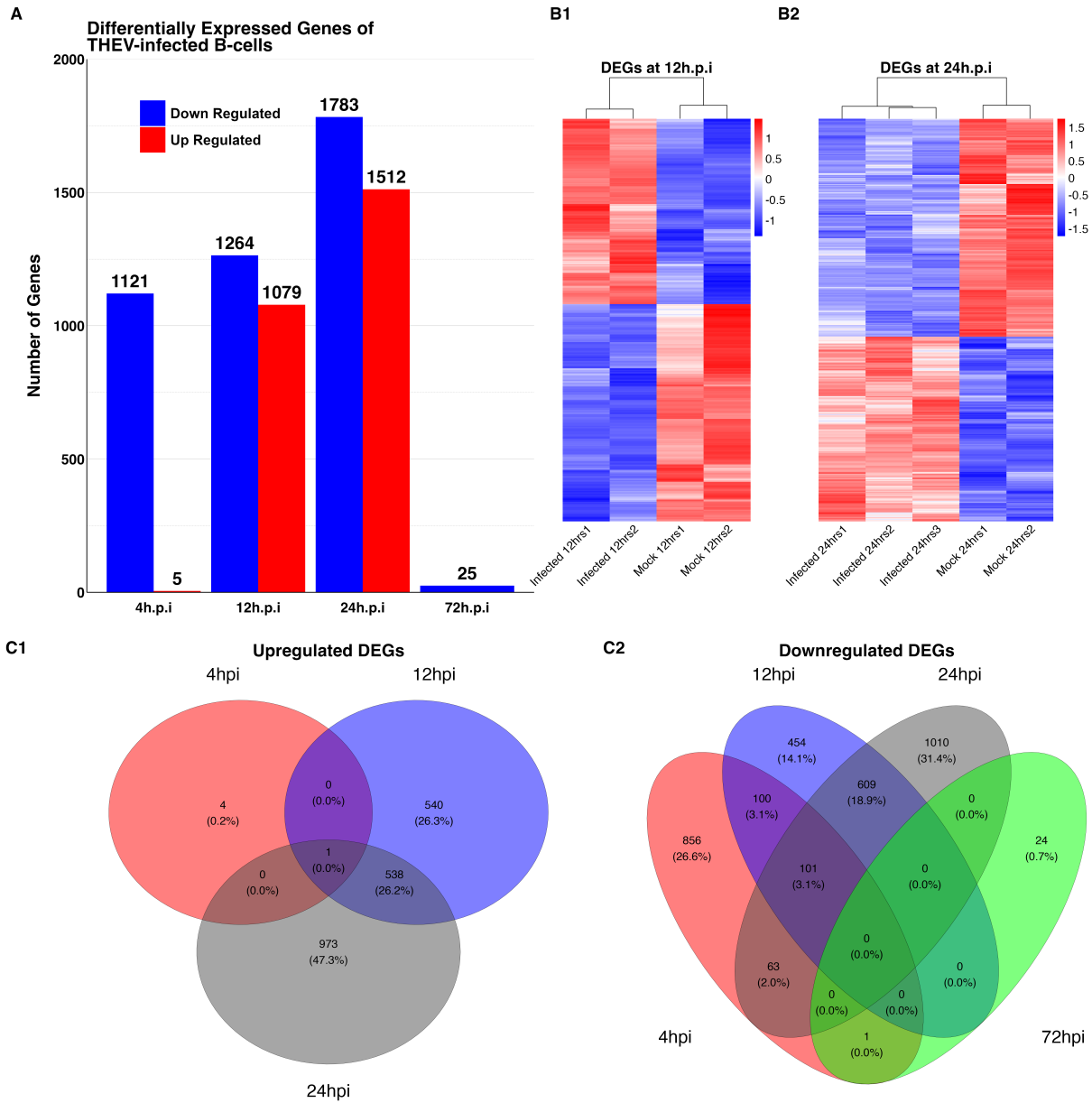
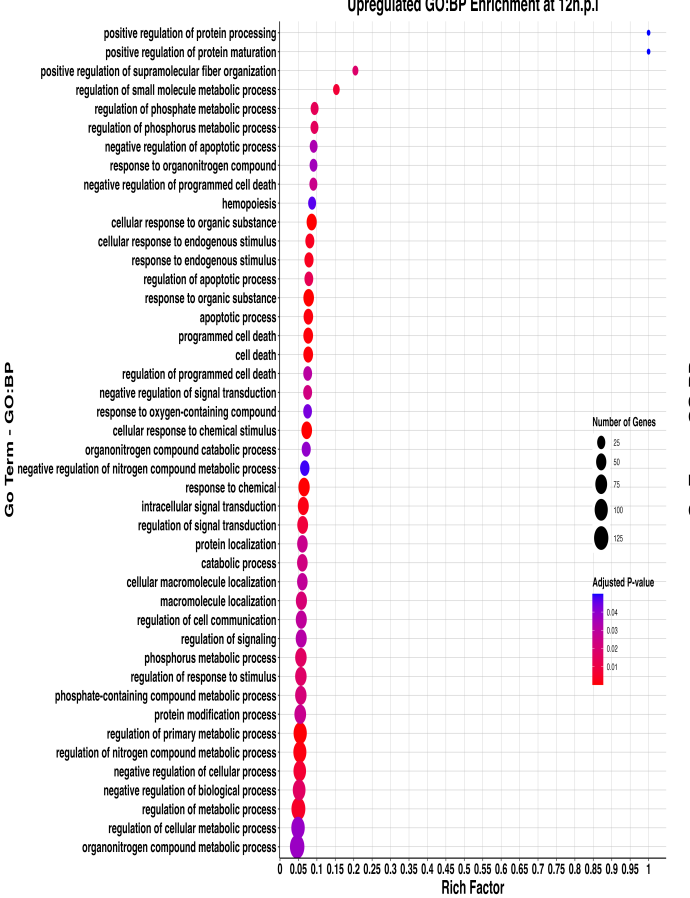
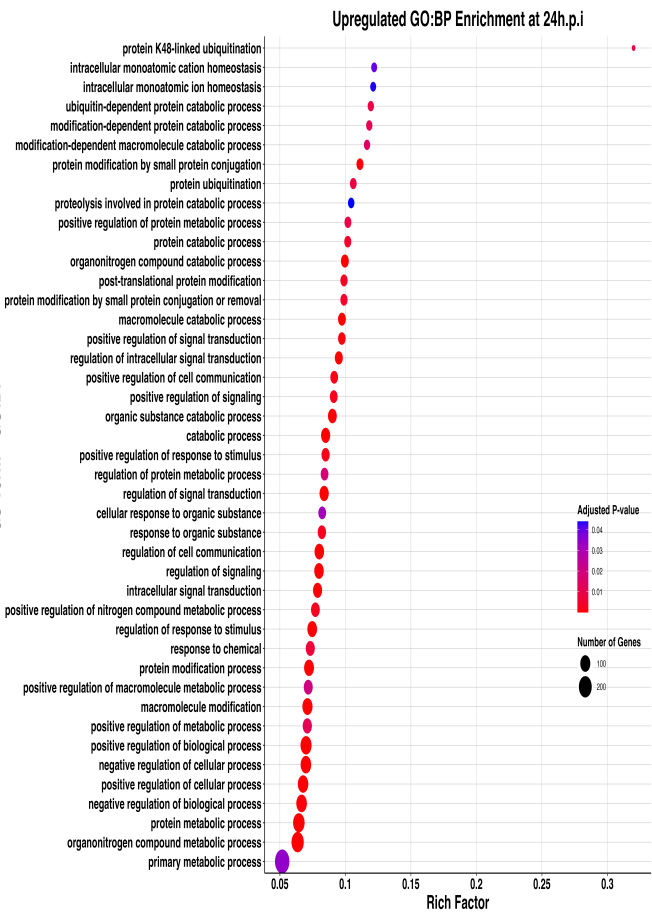


Figure 3: Differentially expressed genes (DEGs) of THEV-infected versus mock-infected samples at different time points. (A) Bar plot of number DEGs identified. Red represents upregulated genes and blue represents downregulated genes. (B) Heatmaps of scaled expression data (Z-scores) of DEGs. DEGs identified at 12-hpi are shown in (B1) and DEGs at 24-hpi in (B2). (C) Venn diagrams showing the number of DEGs identified at different time points. For the upregulated genes (C1), the red circle represents genes at 4-hpi, the blue circle, 12-hpi, and the grey circle, 24-hpi. For the downregulated genes (C2), the green circle represents genes at 72-hpi, while all the other time points retain the colors from (C1).

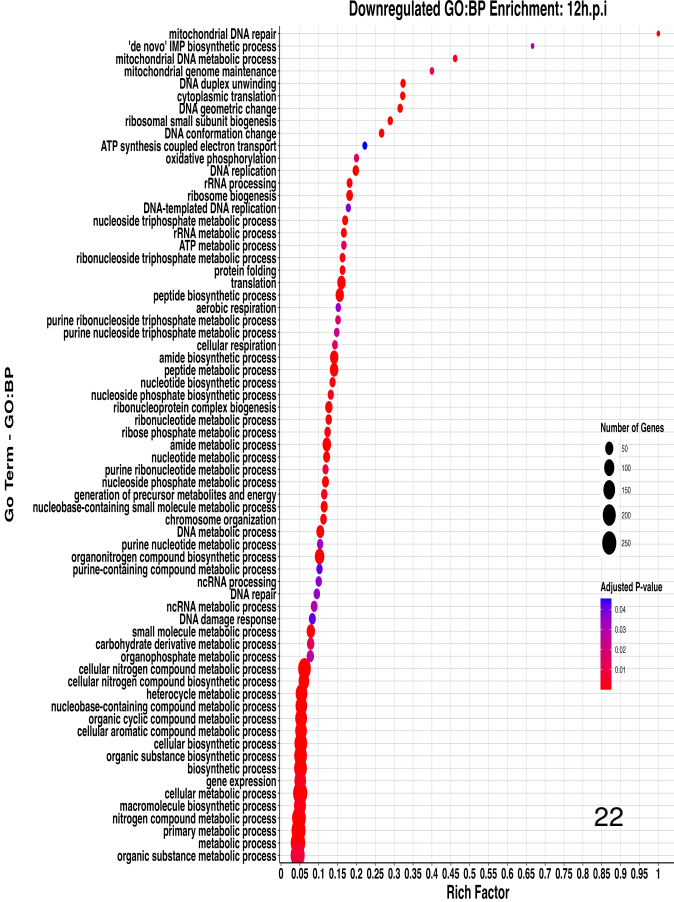
A



B



C



D

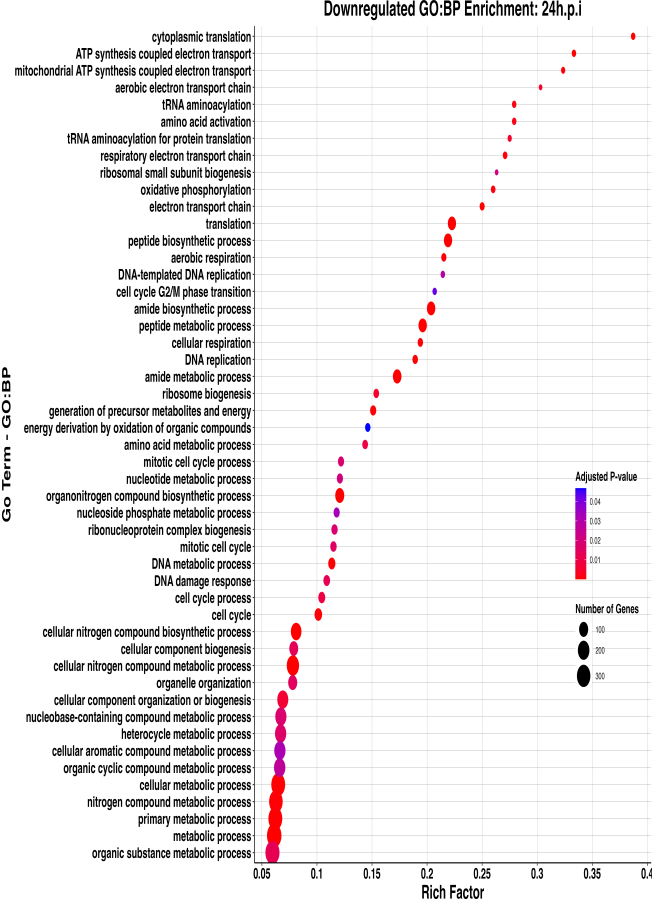


Table 1: Summary of sequencing, quality control, and mapping processes

Sample	Raw Reads ^M	Trimmed Reads ^M	Mapped Reads ^M	Uniquely		Non-uniquely		Q20%	Q30%	GC Content (%)
				Mapped Reads ^M	Mapped Reads ^M	Mapped Reads ^M	Mapped Reads ^M			
I_12hrsS1 ^{Inf}	40.6	39.0	34.7 (88.92%)	33.1 (84.78%)	1.6 (4.14%)	99.95	97.23	47.5		
I_12hrsS3 ^{Inf}	38.8	37.3	33.1 (88.78%)	31.7 (84.95%)	1.4 (3.83%)	99.95	97.53	47.5		
I_24hrsS1 ^{Inf}	42.7	41.0	36.2 (88.13%)	34.5 (84.2%)	1.6 (3.93%)	99.95	96.95	46.5		
I_24hrsS2 ^{Inf}	42.0	40.4	35.6 (88.1%)	33.9 (83.83%)	1.7 (4.27%)	99.94	97.05	46.5		
I_24hrsS3 ^{Inf}	40.5	38.9	34.2 (88.01%)	32.7 (84.12%)	1.5 (3.89%)	99.95	97.08	47.0		
I_4hrsS1 ^{Inf}	39.1	37.4	33 (88.16%)	31.2 (83.43%)	1.8 (4.73%)	99.93	97.04	48.5		
I_4hrsS2 ^{Inf}	41.3	39.6	35.3 (89.24%)	33.6 (84.92%)	1.7 (4.33%)	99.95	97.15	47.0		
I_4hrsS3 ^{Inf}	41.5	39.8	35.5 (89.2%)	33.2 (83.29%)	2.4 (5.91%)	99.95	97.11	47.5		
I_72hrsS1 ^{Inf}	41.2	39.8	28.3 (71.09%)	26.9 (67.7%)	1.3 (3.38%)	99.96	97.23	44.5		
I_72hrsS2 ^{Inf}	39.3	38.0	27 (71.11%)	25.8 (67.86%)	1.2 (3.25%)	99.96	97.34	44.5		
I_72hrsS3 ^{Inf}	39.9	37.1	28.3 (76.36%)	26.1 (70.3%)	2.2 (6.05%)	99.87	96.14	52.5		
U_12hrsN1 ^{Mk}	42.1	40.4	35.9 (88.72%)	34.1 (84.39%)	1.7 (4.33%)	99.95	97.04	47.5		
U_12hrsN2 ^{Mk}	41.0	39.3	34.7 (88.4%)	33.2 (84.53%)	1.5 (3.86%)	99.94	97.08	47.5		
U_24hrsN1 ^{Mk}	38.4	37.0	32.7 (88.46%)	31.4 (84.74%)	1.4 (3.72%)	99.96	97.48	47.5		
U_24hrsN2 ^{Mk}	39.9	38.4	34 (88.58%)	32.6 (84.96%)	1.4 (3.61%)	99.95	96.95	47.0		
U_4hrsN1 ^{Mk}	39.4	37.9	33.7 (88.9%)	32 (84.41%)	1.7 (4.49%)	99.96	97.36	47.0		
U_4hrsN2 ^{Mk}	37.6	34.7	22 (63.43%)	18.5 (53.18%)	3.6 (10.25%)	99.80	94.96	61.0		
U_72hrsN1 ^{Mk}	50.3	47.9	15.5 (32.4%)	11.7 (24.5%)	3.8 (7.9%)	99.88	96.54	56.0		

Sample	Raw Reads ^M	Trimmed Reads ^M	Mapped Reads ^M	Uniquely		Non-uniquely		Q20%	Q30%	GC Content (%)
				Mapped Reads ^M	Mapped Reads ^M	Mapped Reads ^M	Mapped Reads ^M			
U_72hrsN2 ^{Mk}	40.5	38.9	34.5 (88.82%)	32.7 (84.14%)	1.8 (4.68%)	99.95	97.04			46.5

^MAll values for number of reads are in millions;

^{Inf}These are infected samples indicated by the letter 'I' and 'S' in sample names

^{Mk}These are mock-infected samples indicated by the letters 'U' and 'N' in sample names

Table 2A: Gene ontology analysis of Significantly Upregulated DEGs identified at 12-hpi

GO Category	GO:Term	P-value (Adjusted)	Number of DEGs
Biological Process			
GO:BP	cellular response to organic substance	3.38e-06	48
GO:BP	response to organic substance	7.40e-06	55
GO:BP	cellular response to chemical stimulus	6.25e-05	56
GO:BP	response to chemical	1.92e-04	66
GO:BP	regulation of primary metabolic process	3.18e-04	102
GO:BP	cell death	6.58e-04	43
GO:BP	programmed cell death	6.58e-04	43
GO:BP	apoptotic process	1.08e-03	41
GO:BP	regulation of nitrogen compound metabolic process	1.29e-03	98
GO:BP	intracellular signal transduction	1.89e-03	61

GO Category	GO:Term	P-value (Adjusted)	Number of DEGs
GO:BP	response to endogenous stimulus	3.24e-03	36
GO:BP	cellular response to endogenous stimulus	3.27e-03	34
GO:BP	regulation of metabolic process	4.54e-03	116
GO:BP	negative regulation of cellular process	6.47e-03	89
GO:BP	regulation of small molecule metabolic process	7.16e-03	13
GO:BP	regulation of signal transduction	8.44e-03	58
GO:BP	regulation of apoptotic process	1.33e-02	32
GO:BP	regulation of phosphate metabolic process	1.40e-02	23
GO:BP	regulation of phosphorus metabolic process	1.49e-02	23
GO:BP	negative regulation of biological process	1.62e-02	92
GO:BP	phosphorus metabolic process	1.63e-02	69
GO:BP	regulation of response to stimulus	1.73e-02	69
GO:BP	positive regulation of supramolecular fiber organization	1.81e-02	9
GO:BP	macromolecule localization	2.02e-02	63
GO:BP	phosphate-containing compound metabolic process	2.12e-02	68
GO:BP	catabolic process	2.30e-02	55
GO:BP	negative regulation of signal transduction	2.31e-02	33
GO:BP	negative regulation of programmed cell death	2.51e-02	23
GO:BP	protein localization	2.56e-02	54
GO:BP	protein modification process	2.60e-02	73

GO Category	GO:Term	P-value (Adjusted)	Number of DEGs
GO:BP	cellular macromolecule localization	2.81e-02	54
GO:BP	regulation of cell communication	2.87e-02	62
GO:BP	regulation of programmed cell death	3.01e-02	32
GO:BP	regulation of signaling	3.12e-02	62
GO:BP	negative regulation of apoptotic process	3.36e-02	22
GO:BP	response to organonitrogen compound	3.59e-02	22
GO:BP	organonitrogen compound metabolic process	3.75e-02	129
GO:BP	regulation of cellular metabolic process	3.81e-02	106
GO:BP	organonitrogen compound catabolic process	3.92e-02	35
GO:BP	response to oxygen-containing compound	4.31e-02	31
GO:BP	hemopoiesis	4.65e-02	23
GO:BP	negative regulation of nitrogen compound metabolic process	4.83e-02	39
GO:BP	positive regulation of protein processing	5.00e-02	3
GO:BP	positive regulation of protein maturation	5.00e-02	3
Cellular Component			
GO:CC	cytoplasm	5.42e-15	201
GO:CC	intracellular anatomical structure	3.33e-09	253
GO:CC	cytosol	5.72e-09	78
GO:CC	intracellular membrane-bounded organelle	2.13e-06	197
GO:CC	membrane-bounded organelle	5.72e-06	201

GO Category	GO:Term	P-value (Adjusted)	Number of DEGs
GO:CC	intracellular organelle	1.18e-04	218
GO:CC	nucleoplasm	4.02e-04	66
GO:CC	organelle	4.91e-04	219
GO:CC	nucleus	9.73e-04	130
GO:CC	endomembrane system	1.15e-03	75
GO:CC	bounding membrane of organelle	2.72e-03	37
GO:CC	perinuclear region of cytoplasm	4.96e-03	17
GO:CC	organelle membrane	7.16e-03	59
GO:CC	vesicle	7.68e-03	37
GO:CC	cytoplasmic vesicle	2.58e-02	34
GO:CC	intracellular vesicle	2.96e-02	34

Molecular Function

GO:MF	enzyme binding	7.66e-07	50
GO:MF	identical protein binding	1.40e-04	47
GO:MF	protein binding	2.24e-04	192
GO:MF	binding	1.36e-03	302
GO:MF	enzyme regulator activity	2.94e-02	36
GO:MF	small molecule binding	2.96e-02	147
GO:MF	transcription regulator activator activity	4.99e-02	3

Table 2B: Gene ontology analysis of Significantly Downregulated DEGs identified at 12-hpi

GO Category	GO:Term	P-value (Adjusted)	Number of DEGs
Biological Process			
GO:BP	translation	1.67e-17	54
GO:BP	peptide biosynthetic process	6.71e-17	54
GO:BP	peptide metabolic process	1.64e-15	56
GO:BP	organonitrogen compound biosynthetic process	2.83e-15	83
GO:BP	amide biosynthetic process	6.63e-15	54
GO:BP	cellular nitrogen compound metabolic process	1.77e-14	188
GO:BP	amide metabolic process	2.25e-13	59
GO:BP	cellular metabolic process	5.28e-11	254
GO:BP	ribosome biogenesis	1.26e-08	26
GO:BP	DNA replication	8.81e-08	22
GO:BP	ribonucleoprotein complex biogenesis	1.45e-07	35
GO:BP	DNA metabolic process	4.04e-07	44
GO:BP	cellular biosynthetic process	1.11e-06	188
GO:BP	organic substance biosynthetic process	2.66e-06	189
GO:BP	biosynthetic process	3.20e-06	190
GO:BP	cellular nitrogen compound biosynthetic process	6.31e-06	116
GO:BP	DNA geometric change	7.10e-06	12
GO:BP	nucleotide metabolic process	1.84e-05	29

GO Category	GO:Term	P-value (Adjusted)	Number of DEGs
GO:BP	nitrogen compound metabolic process	2.14e-05	232
GO:BP	nucleobase-containing small molecule metabolic process	2.14e-05	31
GO:BP	DNA duplex unwinding	2.32e-05	11
GO:BP	heterocycle metabolic process	2.81e-05	150
GO:BP	nucleoside phosphate metabolic process	3.22e-05	29
GO:BP	primary metabolic process	5.30e-05	244
GO:BP	small molecule metabolic process	5.59e-05	55
GO:BP	DNA conformation change	5.96e-05	12
GO:BP	organic cyclic compound metabolic process	7.26e-05	153
GO:BP	ribosomal small subunit biogenesis	8.54e-05	11
GO:BP	metabolic process	1.02e-04	267
GO:BP	nucleobase-containing compound metabolic process	1.06e-04	145
GO:BP	cytoplasmic translation	1.07e-04	10
GO:BP	rRNA processing	1.28e-04	16
GO:BP	nucleoside triphosphate metabolic process	1.43e-04	17
GO:BP	cellular aromatic compound metabolic process	1.90e-04	148
GO:BP	rRNA metabolic process	4.46e-04	16
GO:BP	ribonucleotide metabolic process	4.77e-04	22
GO:BP	ribose phosphate metabolic process	7.10e-04	22
GO:BP	nucleotide biosynthetic process	8.95e-04	19

GO Category	GO:Term	P-value (Adjusted)	Number of DEGs
GO:BP	chromosome organization	1.21e-03	24
GO:BP	protein folding	1.38e-03	15
GO:BP	ribonucleoside triphosphate metabolic process	1.38e-03	15
GO:BP	nucleoside phosphate biosynthetic process	1.55e-03	19
GO:BP	macromolecule biosynthetic process	1.69e-03	159
GO:BP	mitochondrial DNA repair	2.13e-03	4
GO:BP	gene expression	2.39e-03	149
GO:BP	generation of precursor metabolites and energy	2.59e-03	22
GO:BP	mitochondrial DNA metabolic process	3.90e-03	6
GO:BP	organic substance metabolic process	6.79e-03	250
GO:BP	purine ribonucleotide metabolic process	8.33e-03	19
GO:BP	mitochondrial genome maintenance	1.07e-02	6
GO:BP	carbohydrate derivative metabolic process	1.23e-02	37
GO:BP	ATP metabolic process	1.29e-02	12
GO:BP	oxidative phosphorylation	1.33e-02	10
GO:BP	cellular respiration	1.54e-02	14
GO:BP	purine ribonucleoside triphosphate metabolic process	1.68e-02	13
GO:BP	purine nucleoside triphosphate metabolic process	2.17e-02	13
GO:BP	organophosphate metabolic process	2.67e-02	35
GO:BP	ncRNA metabolic process	2.90e-02	27

GO Category	GO:Term	P-value (Adjusted)	Number of DEGs
GO:BP	'de novo' IMP biosynthetic process	3.01e-02	4
GO:BP	purine nucleotide metabolic process	3.37e-02	20
GO:BP	aerobic respiration	3.42e-02	12
GO:BP	DNA repair	3.48e-02	23
GO:BP	ncRNA processing	3.64e-02	21
GO:BP	DNA-templated DNA replication	3.78e-02	10
GO:BP	DNA damage response	4.19e-02	29
GO:BP	purine-containing compound metabolic process	4.21e-02	20
GO:BP	ATP synthesis coupled electron transport	4.54e-02	8
Cellular Component			
GO:CC	intracellular anatomical structure	2.34e-20	315
GO:CC	protein-containing complex	2.35e-19	177
GO:CC	ribosomal subunit	6.90e-19	28
GO:CC	cytosolic ribosome	2.02e-18	21
GO:CC	ribosome	4.82e-16	39
GO:CC	intracellular organelle	4.96e-16	284
GO:CC	cytosolic large ribosomal subunit	1.59e-15	15
GO:CC	ribonucleoprotein complex	4.59e-15	62
GO:CC	organelle	2.14e-14	284
GO:CC	intracellular membrane-bounded organelle	1.66e-12	245

GO Category	GO:Term	P-value (Adjusted)	Number of DEGs
GO:CC	large ribosomal subunit	9.19e-12	18
GO:CC	membrane-bounded organelle	1.37e-10	246
GO:CC	organelle lumen	1.92e-10	118
GO:CC	intracellular organelle lumen	1.92e-10	118
GO:CC	membrane-enclosed lumen	1.92e-10	118
GO:CC	envelope	8.50e-10	47
GO:CC	organelle envelope	8.50e-10	47
GO:CC	nucleus	2.90e-09	169
GO:CC	cytoplasm	4.68e-09	212
GO:CC	intracellular non-membrane-bounded organelle	5.50e-09	135
GO:CC	non-membrane-bounded organelle	5.50e-09	135
GO:CC	mitochondrion	6.70e-09	58
GO:CC	mitochondrial inner membrane	7.34e-08	26
GO:CC	organelle inner membrane	1.42e-07	27
GO:CC	nuclear lumen	1.69e-07	103
GO:CC	mitochondrial envelope	6.30e-07	32
GO:CC	mitochondrial membrane	1.15e-06	30
GO:CC	small ribosomal subunit	2.19e-06	10
GO:CC	mitochondrial protein-containing complex	1.13e-05	20
GO:CC	respirasome	3.77e-05	12

GO Category	GO:Term	P-value (Adjusted)	Number of DEGs
GO:CC	inner mitochondrial membrane protein complex	5.48e-05	14
GO:CC	respiratory chain complex	8.15e-05	11
GO:CC	catalytic complex	8.42e-05	55
GO:CC	cytosol	1.29e-04	75
GO:CC	preribosome	1.72e-04	10
GO:CC	cytosolic small ribosomal subunit	1.76e-04	6
GO:CC	respiratory chain complex I	2.46e-04	8
GO:CC	NADH dehydrogenase complex	2.46e-04	8
GO:CC	mitochondrial respirasome	2.85e-04	10
GO:CC	protein folding chaperone complex	3.55e-04	7
GO:CC	oxidoreductase complex	3.58e-04	12
GO:CC	nucleoplasm	5.96e-04	74
GO:CC	chaperonin-containing T-complex	1.70e-03	4
GO:CC	small-subunit processome	2.12e-03	8
GO:CC	nucleolus	2.15e-03	41
GO:CC	mitochondrial respiratory chain complex I	2.34e-03	7
GO:CC	chromosome	8.26e-03	37
GO:CC	organelle membrane	1.24e-02	66
GO:CC	nuclear protein-containing complex	1.93e-02	40
GO:CC	Ctf18 RFC-like complex	3.81e-02	3

GO Category	GO:Term	P-value (Adjusted)	Number of DEGs
GO:CC	eukaryotic translation initiation factor 3 complex, eIF3m	3.81e-02	3
GO:CC	eukaryotic 48S preinitiation complex	3.82e-02	4
GO:CC	rough endoplasmic reticulum	3.92e-02	5
Molecular Function			
GO:MF	structural constituent of ribosome	1.10e-15	35
GO:MF	organic cyclic compound binding	1.33e-09	171
GO:MF	nucleic acid binding	1.13e-06	101
GO:MF	RNA binding	1.46e-06	52
GO:MF	structural molecule activity	3.18e-06	41
GO:MF	DNA helicase activity	2.69e-05	9
GO:MF	unfolded protein binding	3.20e-05	11
GO:MF	ATP hydrolysis activity	3.51e-05	24
GO:MF	catalytic activity, acting on a nucleic acid	5.60e-05	34
GO:MF	translation regulator activity	1.25e-04	13
GO:MF	catalytic activity, acting on DNA	2.97e-04	18
GO:MF	heterocyclic compound binding	4.39e-04	88
GO:MF	nucleoside phosphate binding	7.58e-04	84
GO:MF	nucleotide binding	7.58e-04	84
GO:MF	protein folding chaperone	9.92e-04	9
GO:MF	adenyl nucleotide binding	1.16e-03	68

GO Category	GO:Term	P-value (Adjusted)	Number of DEGs
GO:MF	ATP-dependent protein folding chaperone	1.38e-03	8
GO:MF	purine nucleotide binding	3.23e-03	78
GO:MF	ATP-dependent activity, acting on DNA	3.67e-03	12
GO:MF	hydrolase activity, acting on acid anhydrides	7.09e-03	33
GO:MF	ribonucleoprotein complex binding	7.21e-03	11
GO:MF	ATP-dependent activity	7.43e-03	31
GO:MF	translation regulator activity, nucleic acid binding	7.88e-03	10
GO:MF	anion binding	1.10e-02	83
GO:MF	helicase activity	1.39e-02	12
GO:MF	pyrophosphatase activity	1.47e-02	32
GO:MF	NAD binding	1.64e-02	8
GO:MF	hydrolase activity, acting on acid anhydrides, in phosphorus-containing anhydrides	1.67e-02	32
GO:MF	translation factor activity, RNA binding	2.37e-02	9
GO:MF	ribonucleoside triphosphate phosphatase activity	2.53e-02	30
GO:MF	hydroxymethyl-, formyl- and related transferase activity	2.61e-02	4
GO:MF	mRNA binding	4.75e-02	12

Table 3A: Gene ontology analysis of Significantly Upregulated DEGs identified at 24-hpi

GO Category	GO:Term	P-value (Adjusted)	Number of DEGs
Biological Process			
GO:BP	positive regulation of biological process	4.76e-06	133
GO:BP	organonitrogen compound metabolic process	7.66e-06	176
GO:BP	organic substance catabolic process	8.02e-06	68
GO:BP	catabolic process	9.68e-06	77
GO:BP	regulation of signal transduction	1.08e-05	79
GO:BP	regulation of cell communication	1.78e-05	86
GO:BP	regulation of signaling	2.03e-05	86
GO:BP	organonitrogen compound catabolic process	6.25e-05	49
GO:BP	negative regulation of cellular process	8.39e-05	116
GO:BP	protein metabolic process	1.17e-04	148
GO:BP	regulation of intracellular signal transduction	1.51e-04	51
GO:BP	macromolecule catabolic process	1.74e-04	48
GO:BP	regulation of response to stimulus	1.79e-04	91
GO:BP	macromolecule modification	2.23e-04	104
GO:BP	intracellular signal transduction	2.96e-04	76
GO:BP	protein modification process	3.57e-04	96
GO:BP	positive regulation of cellular process	5.36e-04	115
GO:BP	protein modification by small protein conjugation	6.56e-04	34

GO Category	GO:Term	P-value (Adjusted)	Number of DEGs
GO:BP	positive regulation of signal transduction	8.37e-04	43
GO:BP	negative regulation of biological process	8.76e-04	118
GO:BP	positive regulation of response to stimulus	1.83e-03	55
GO:BP	positive regulation of cell communication	1.92e-03	46
GO:BP	positive regulation of signaling	2.15e-03	46
GO:BP	response to organic substance	2.75e-03	58
GO:BP	positive regulation of nitrogen compound metabolic process	3.07e-03	68
GO:BP	post-translational protein modification	3.53e-03	37
GO:BP	protein catabolic process	4.85e-03	34
GO:BP	protein modification by small protein conjugation or removal	4.88e-03	36
GO:BP	response to chemical	7.06e-03	74
GO:BP	protein ubiquitination	8.16e-03	30
GO:BP	protein K48-linked ubiquitination	9.05e-03	8
GO:BP	positive regulation of protein metabolic process	9.19e-03	32
GO:BP	ubiquitin-dependent protein catabolic process	9.45e-03	24
GO:BP	modification-dependent protein catabolic process	1.12e-02	24
GO:BP	positive regulation of metabolic process	1.23e-02	78
GO:BP	modification-dependent macromolecule catabolic process	1.44e-02	24
GO:BP	regulation of protein metabolic process	1.81e-02	46
GO:BP	positive regulation of macromolecule metabolic process	2.04e-02	72

GO Category	GO:Term	P-value (Adjusted)	Number of DEGs
GO:BP	cellular response to organic substance	3.15e-02	46
GO:BP	primary metabolic process	3.44e-02	272
GO:BP	intracellular monoatomic cation homeostasis	3.99e-02	20
GO:BP	intracellular monoatomic ion homeostasis	4.37e-02	20
GO:BP	proteolysis involved in protein catabolic process	4.40e-02	26
Cellular Component			
GO:CC	cytoplasm	6.93e-15	268
GO:CC	intracellular anatomical structure	8.47e-08	343
GO:CC	intracellular membrane-bounded organelle	7.95e-07	270
GO:CC	cytosol	3.71e-06	92
GO:CC	membrane-bounded organelle	7.07e-06	274
GO:CC	organelle membrane	1.00e-05	88
GO:CC	endomembrane system	1.94e-05	106
GO:CC	intracellular organelle	3.19e-04	298
GO:CC	organelle	1.28e-03	300
GO:CC	perinuclear region of cytoplasm	1.51e-03	22
GO:CC	bounding membrane of organelle	4.31e-03	47
GO:CC	nucleoplasm	6.28e-03	82
GO:CC	Golgi apparatus	2.20e-02	44
GO:CC	vacuole	2.85e-02	21

GO Category	GO:Term	P-value (Adjusted)	Number of DEGs
GO:CC	vacuolar membrane	4.14e-02	15
Molecular Function			
GO:MF	acyltransferase activity	7.50e-04	34
GO:MF	aminoacyltransferase activity	9.34e-04	24
GO:MF	ubiquitin-like protein ligase activity	1.68e-03	17
GO:MF	transferase activity	2.20e-03	101
GO:MF	small molecule binding	3.46e-03	187
GO:MF	ubiquitin-like protein transferase activity	4.36e-03	22
GO:MF	ubiquitin protein ligase activity	4.44e-03	16
GO:MF	adenyl nucleotide binding	4.80e-03	80
GO:MF	adenyl ribonucleotide binding	5.52e-03	76
GO:MF	ATP binding	5.94e-03	75
GO:MF	ubiquitin-protein transferase activity	7.85e-03	21
GO:MF	catalytic activity, acting on a protein	9.55e-03	95
GO:MF	active monoatomic ion transmembrane transporter activity	1.37e-02	17
GO:MF	protein phosphorylated amino acid binding	1.61e-02	7
GO:MF	phosphotyrosine residue binding	4.95e-02	6
GO:MF	ion binding	4.98e-02	176

Table 3B: Gene ontology analysis of Significantly Downregulated DEGs identified at 24-hpi

GO Category	GO:Term	P-value (Adjusted)	Number of DEGs
Biological Process			
GO:BP	translation	1.81e-25	75
GO:BP	peptide biosynthetic process	2.30e-25	76
GO:BP	amide biosynthetic process	6.94e-24	78
GO:BP	peptide metabolic process	9.87e-23	78
GO:BP	amide metabolic process	8.33e-21	84
GO:BP	organonitrogen compound biosynthetic process	3.71e-13	98
GO:BP	cellular nitrogen compound metabolic process	1.11e-11	236
GO:BP	cellular nitrogen compound biosynthetic process	5.35e-07	155
GO:BP	cellular metabolic process	6.87e-07	324
GO:BP	cytoplasmic translation	2.39e-05	12
GO:BP	metabolic process	2.89e-05	364
GO:BP	electron transport chain	1.28e-04	16
GO:BP	primary metabolic process	1.46e-04	327
GO:BP	ATP synthesis coupled electron transport	1.67e-04	12
GO:BP	generation of precursor metabolites and energy	2.04e-04	29
GO:BP	DNA metabolic process	2.19e-04	48
GO:BP	DNA replication	2.40e-04	21
GO:BP	nitrogen compound metabolic process	3.91e-04	306

GO Category	GO:Term	P-value (Adjusted)	Number of DEGs
GO:BP	aerobic respiration	5.32e-04	17
GO:BP	cell cycle	5.70e-04	58
GO:BP	cellular respiration	6.24e-04	19
GO:BP	respiratory electron transport chain	7.64e-04	13
GO:BP	mitochondrial ATP synthesis coupled electron transport	8.01e-04	11
GO:BP	oxidative phosphorylation	1.28e-03	13
GO:BP	amino acid activation	1.47e-03	12
GO:BP	tRNA aminoacylation	1.47e-03	12
GO:BP	ribosome biogenesis	4.83e-03	22
GO:BP	tRNA aminoacylation for protein translation	4.88e-03	11
GO:BP	aerobic electron transport chain	5.18e-03	10
GO:BP	cellular component organization or biogenesis	6.34e-03	173
GO:BP	cell cycle process	9.13e-03	43
GO:BP	amino acid metabolic process	9.43e-03	23
GO:BP	DNA damage response	1.21e-02	38
GO:BP	organic substance metabolic process	1.27e-02	338
GO:BP	cellular component biogenesis	1.37e-02	94
GO:BP	organelle organization	1.43e-02	98
GO:BP	mitotic cell cycle	1.54e-02	33
GO:BP	heterocycle metabolic process	1.65e-02	185

GO Category	GO:Term	P-value (Adjusted)	Number of DEGs
GO:BP	mitotic cell cycle process	1.75e-02	29
GO:BP	ribonucleoprotein complex biogenesis	1.77e-02	32
GO:BP	nucleobase-containing compound metabolic process	1.78e-02	181
GO:BP	nucleotide metabolic process	2.06e-02	29
GO:BP	ribosomal small subunit biogenesis	2.10e-02	10
GO:BP	organic cyclic compound metabolic process	2.68e-02	190
GO:BP	DNA-templated DNA replication	2.91e-02	12
GO:BP	cellular aromatic compound metabolic process	3.19e-02	185
GO:BP	nucleoside phosphate metabolic process	3.30e-02	29
GO:BP	cell cycle G2/M phase transition	4.23e-02	12
GO:BP	energy derivation by oxidation of organic compounds	4.68e-02	19

Cellular Component

GO:CC	intracellular anatomical structure	1.68e-21	430
GO:CC	cytosolic ribosome	1.59e-19	24
GO:CC	ribosome	1.12e-17	48
GO:CC	protein-containing complex	1.59e-17	225
GO:CC	intracellular organelle	6.94e-17	386
GO:CC	cytosolic large ribosomal subunit	9.52e-17	17
GO:CC	ribosomal subunit	7.01e-16	29
GO:CC	organelle	1.29e-15	388

GO Category	GO:Term	P-value (Adjusted)	Number of DEGs
GO:CC	mitochondrion	3.64e-13	82
GO:CC	non-membrane-bounded organelle	2.70e-12	188
GO:CC	intracellular non-membrane-bounded organelle	2.70e-12	188
GO:CC	ribonucleoprotein complex	2.14e-11	69
GO:CC	large ribosomal subunit	2.57e-11	20
GO:CC	cytoplasm	9.78e-11	291
GO:CC	membrane-bounded organelle	8.65e-08	322
GO:CC	intracellular membrane-bounded organelle	1.46e-07	312
GO:CC	organelle lumen	2.56e-07	143
GO:CC	intracellular organelle lumen	2.56e-07	143
GO:CC	membrane-enclosed lumen	2.56e-07	143
GO:CC	respirasome	5.31e-07	16
GO:CC	catalytic complex	5.79e-07	77
GO:CC	mitochondrial respirasome	1.57e-06	14
GO:CC	mitochondrial inner membrane	1.78e-06	29
GO:CC	nucleoplasm	1.94e-06	106
GO:CC	respiratory chain complex	6.15e-06	14
GO:CC	oxidoreductase complex	1.20e-05	16
GO:CC	organelle inner membrane	1.80e-05	29
GO:CC	cytosol	1.90e-05	101

GO Category	GO:Term	P-value (Adjusted)	Number of DEGs
GO:CC	nuclear lumen	1.95e-05	127
GO:CC	mitochondrial membrane	2.93e-05	34
GO:CC	nucleus	3.43e-05	208
GO:CC	mitochondrial envelope	8.32e-05	35
GO:CC	chromosome	1.20e-04	53
GO:CC	inner mitochondrial membrane protein complex	1.38e-04	16
GO:CC	mitochondrial protein-containing complex	2.05e-04	22
GO:CC	envelope	5.02e-04	45
GO:CC	organelle envelope	5.02e-04	45
GO:CC	small ribosomal subunit	7.43e-04	9
GO:CC	cytosolic small ribosomal subunit	1.52e-03	6
GO:CC	respiratory chain complex I	3.69e-03	8
GO:CC	NADH dehydrogenase complex	3.69e-03	8
GO:CC	chromosomal region	5.59e-03	20
GO:CC	mitochondrial respiratory chain complex I	2.48e-02	7
GO:CC	chromosome, centromeric region	2.55e-02	15
GO:CC	preribosome	2.79e-02	9
GO:CC	condensed chromosome	3.62e-02	15
GO:CC	chromatin	4.43e-02	29
GO:CC	protein-DNA complex	4.56e-02	31

GO Category	GO:Term	P-value (Adjusted)	Number of DEGs
Molecular Function			
GO:MF	structural constituent of ribosome	5.85e-16	42
GO:MF	structural molecule activity	2.04e-06	53
GO:MF	nucleic acid binding	4.11e-06	134
GO:MF	translation regulator activity	9.31e-06	17
GO:MF	catalytic activity, acting on a nucleic acid	9.93e-05	43
GO:MF	organic cyclic compound binding	1.05e-04	214
GO:MF	RNA binding	3.34e-04	61
GO:MF	catalytic activity, acting on DNA	4.35e-04	22
GO:MF	ligase activity	8.09e-04	20
GO:MF	aminoacyl-tRNA ligase activity	1.05e-03	11
GO:MF	ligase activity, forming carbon-oxygen bonds	1.05e-03	11
GO:MF	translation regulator activity, nucleic acid binding	1.75e-03	13
GO:MF	translation factor activity, RNA binding	3.82e-03	12
GO:MF	NAD binding	4.94e-02	9

Table 4A: Significantly Enriched KEGG Pathways from DEGs identified at 12 and 24-hpi (Results from the DAVID online resource)

Time Point	Regulation	KEGG Term	DEG Count	Fold Enrichment	P-value (Adjusted)
12-hpi	down	Ribosome	80	6.68	3.16e-49
12-hpi	down	Oxidative phosphorylation	37	3.22	1.08e-08
12-hpi	down	DNA replication	18	6.01	1.09e-08
12-hpi	down	Ribosome biogenesis in eukaryotes	27	4.03	1.09e-08
12-hpi	down	Spliceosome	30	2.50	1.25e-04
12-hpi	down	Nucleocytoplasmic transport	22	2.29	1.00e-02
12-hpi	down	Base excision repair	13	3.10	1.13e-02
12-hpi	down	Mismatch repair	9	4.29	1.13e-02
12-hpi	down	Nucleotide excision repair	14	2.86	1.29e-02
12-hpi	up	Steroid biosynthesis	10	6.14	1.65e-03
12-hpi	up	Autophagy - animal	29	2.34	2.12e-03
12-hpi	up	Cell cycle	27	2.30	3.90e-03
12-hpi	up	Influenza A	22	2.13	4.74e-02
24-hpi	down	Ribosome	88	5.54	2.81e-49
24-hpi	down	Oxidative phosphorylation	50	3.28	2.71e-13
24-hpi	down	Carbon metabolism	39	2.98	1.08e-08
24-hpi	down	Aminoacyl-tRNA biosynthesis	22	3.78	1.10e-06
24-hpi	down	Biosynthesis of amino acids	24	3.02	2.50e-05

Table 4A: Significantly Enriched KEGG Pathways from DEGs identified at 12 and 24-hpi (Results from the DAVID online resource)

Time Point	Regulation	KEGG Term	DEG Count	Fold Enrichment	P-value (Adjusted)
24-hpi	down	Citrate cycle (TCA cycle)	15	4.36	2.50e-05
24-hpi	down	DNA replication	15	3.78	1.93e-04
24-hpi	down	Spliceosome	33	2.08	1.09e-03
24-hpi	down	Metabolic pathways	225	1.22	3.04e-03
24-hpi	down	Cell cycle	36	1.89	3.04e-03
24-hpi	down	Propanoate metabolism	12	3.24	7.53e-03
24-hpi	down	Fatty acid degradation	14	2.86	7.77e-03
24-hpi	down	Glycolysis / Gluconeogenesis	17	2.42	1.19e-02
24-hpi	down	One carbon pool by folate	9	3.78	1.35e-02
24-hpi	down	Nucleotide excision repair	15	2.31	3.73e-02
24-hpi	down	Pyruvate metabolism	12	2.59	4.20e-02
24-hpi	up	Steroid biosynthesis	11	5.15	1.92e-03
24-hpi	up	Lysosome	29	2.24	3.94e-03
24-hpi	up	Terpenoid backbone biosynthesis	9	4.43	1.73e-02
24-hpi	up	Glycosaminoglycan biosynthesis - heparan sulfate / heparin	10	3.90	1.73e-02
24-hpi	up	Protein processing in endoplasmic reticulum	30	1.94	1.73e-02
24-hpi	up	Autophagy - animal	30	1.85	3.19e-02

Table 4B: Significantly Enriched KEGG Pathways from DEGs identified at 12 and 24-hpi (Results from the gprofiler2 R package)

Time Point	Regulation	KEGG Term	DEG Count	P-value (Adjusted)
12-hpi	down	Ribosome	35	7.70e-24
12-hpi	down	DNA replication	11	5.07e-07
12-hpi	down	Oxidative phosphorylation	19	3.10e-04
12-hpi	down	Base excision repair	9	1.15e-03
12-hpi	down	One carbon pool by folate	6	1.27e-03
12-hpi	down	Mismatch repair	6	3.49e-03
12-hpi	down	Ribosome biogenesis in eukaryotes	9	1.77e-02
12-hpi	down	Nucleotide excision repair	8	3.36e-02
12-hpi	up	Autophagy - animal	13	2.09e-02
24-hpi	down	Ribosome	41	4.71e-28
24-hpi	down	Aminoacyl-tRNA biosynthesis	12	3.04e-04
24-hpi	down	Oxidative phosphorylation	22	4.35e-04
24-hpi	down	Base excision repair	9	1.15e-02
24-hpi	down	Carbon metabolism	14	3.14e-02
24-hpi	down	Propanoate metabolism	6	3.99e-02
24-hpi	up	Ubiquitin mediated proteolysis	17	7.26e-03
24-hpi	up	Steroid biosynthesis	5	2.63e-02

253 **SUPPLEMENTARY INFORMATION/MATERIALS**